P-ISSN 2586-9000
E-ISSN 2586-9027

Homepage : https://tci-thaijo.org/index.php/SciTechAsia

Science & Technology Asia

Vol. 26 No.4 October - December 2021

Page: [59-73]

Original research article

Mathematical Study of MHD Casson Fluid Flow through Porous Media along with Soret and Dufour Effects Over a Stretching Surface

Ruchi Jain[1], Ruchika Mehta[1,*], Tripti Mehta[2], Sushila[3]

[1]*Department of Mathematics & Statistics, Manipal University Jaipur, Jaipur 303007, India*
[2]*Department of Mathematics, S.S. Jain Subodh P.G. College, Jaipur 302007, India*
[3]*Department of Physics, Vivekananda Global University, Jaipur 303012, India*

Received 02 August 2021; Received in revised form 14 November 2021
Accepted 25 November 2021; Available online 30 December 2021

ABSTRACT:

In this paper multiple slip effects are investigated over inclined permeable extending lamina as well as on melting surface for the MHD non-Newtonian Casson fluid. We analysed the effect of first and second order velocity and concentration slip along with the Soret and Dufour effect. Viscous dissipation, nonlinear heat radiation from a nonlinear heat source is taken. The fluid is having a nonlinear chemical reaction. All the three governing equations of motion, heat and concentration are analysed and solved by bvp4c MATLAB solver. In this investigation we find the impact on different physical parameters and describe them in the form of graphs. Also the table is formed for the values of skin friction, Nusselt number and Sherwood coefficient.

Keywords: Chemically reactive; Casson fluid flow; Magnetic field; Multiple slip; Porous media.

1. Introduction

The word MHD is used initially by the HannesAlfven in 1942. MHD is basically regarded as the steady of magnetic behaviour and properties of electro-conducting fluid. It is widely used in the areas where heat transmission takes place through electrically conducting fluid like plasma propulsion, thrusters etc. Andersson et al. examined the effect of chemical reaction of diffusion of species [1]. Impact of viscosity of a MHD UCM fluid passing through extending lamina with internal heat absorption or generation is examined by

***Corresponding author:** ruchika.mehta1981@gmail.com **doi:** 10.14456/scitechasia.2021.66

Prasad et al. [2]. Bhattacharyya analysed the effect of heat transfer of non-Newtonian (Casson) fluid flowing in the direction of extending lamina. An UCM Maxwell fluid is analysed for the effect of chemical reaction moving through extending sheet by Mukhopadhyay et al. [3]. The nano fluid over a two-dimensional expending lamina is analysed for different physical properties by Nadeem and Hussain [4]. Casson fluid is a non-Newtonian fluid which is considered to be a shear thing liquid having infinite viscosity when the shear rate is assumed to be zero. Casson fluid model is useful in many studies related to blood flow. It is also useful in the manufacturing of pharmaceutical products, coal in water, China clay, paints, synthetic lubricants, and biological fluids such as synovial fluids, sewage sludge, jelly, tomato sauce, honey, soup. Kumar and Gangadhar analysed the effect of viscous dissipation on MHD Casson fluid over a extending lamina along with the velocity and temperature slip [5]. Kumar and Gangadhar examined the effect of MHD on Casson fluid flowing over a extending lamina with heat transfer and mass transfer [6]. Properties of Casson fluid are studied under the effect of slip flow and Heat and mass transfer by Megahed [7]. Nadeem et al. detected the different properties of mixed fluid (water and kerosene) having nano particles of cu on a convective plane [8]. Slip boundary conditions are applied over Casson fluid and investigated the basic flows of fluid by Ramesh et al. [9]. Kataria and Patel studied Casson fluid flow with Soret and Dufour effect over a plate oscillating vertically placed in porous media [10]. Nagendramma et.al. studied the Maxwell fluid flow with heat and mass transformation and various properties [11].

Casson fluid with induced magnetic effect is analysed by Raju et al. [12]. Brownian motion is applied over a extending surface is examined for the MHD fluid (Newtonian-Non-Newtonian)by Sulochana et al. [13]. Krishnamurthy et al. considered a MHD Non-Newtonian Williamson fluid on a upstanding lamina [14]. Non-Newtonian fluid is taken into consideration for various physical properties and explained their effect on fluid by Jain et al. [15-18]. Raju et al. analysed flow of a casson fluid on a sheet of variable thickness along with multiple slip [19]. Parmar scrutinised the effect of falkner-skan flow over a moving plate of a non-Newtonian fluid [20]. A nano fluid flow is examined by Rajni et al. for the effect of higher order chemical reaction and slip condition [21]. Ferro-fluid over a non-linear porous sheet with multiple slip is examined by Sivakumar et al. [22]. MHD fluid flow over a upstanding moving permeable plate with chemical reaction is analysed by Arifuzzaman [23]. Casson fluid over a contracting plane are studied for the MHD flow with slip effect and suction in presence of chemical reaction by Yahaya et al. [24]. Ajala et al. analysed the effect of MHD nano fluid flow over a out cover of arevolutionary paraboloid [25]. Das et al. gives a study of heat and mass transfer effect on MHD Casson fluid flowing through porous channel in addition to double diffusivity [26]. Hybrid fluid with nano particles is studied by Waini et al. on a contracting lamina for analysing the effect of temperature transformation [27]. Asogwa and Ibe examined effect of heat and mass transfer on Casson fluid flowing through porous extending lamina [28]. Hafidzuddinanalysed slip boundary and suction effect on a MHD Casson fluid [29]. Khan et al. made research to study the effect of radiative three-dimensional flow of a liquid with Ti_6Al_4V alloy nano particles [30]. UCM fluid is analysed by Palani et al. over a extending lamina of variable thickness with applied magnetic effect [31]. Rassool et al. scrutinized the Darcy Forchheimer fluid with nano particle for different properties like entropy analysis [32]. The researcher investigates the result on behaviour of Casson fluid flowing through exponentially extending lamina with heat and mass transfer and buoyancy parameters by Parvin [1]. Bilal et al. analysed the flow of a Newtonian fluid over a disk rotating with Ω velocity for the Heat and mass transfer effect [33]. Hussain et al. examined various time dependent properties of non-Newtonian liquid [34]. Jamshed et al. study the single-phase model of Casson fluid [35]. Lie scaling approach was used by Saleem for the MHD fluid over a stiff lamina [36]. Shoaib et al. go through the Re-Eyring fluid model [37].

This particular investigation deals with Casson fluid model having two boundary conditions along with Soretand Dufour effect and applied magnetic field. This study is the extension of the problem proposed by Jain and Parmar [38]. The results are useful for the students interested in the study of manufacturing of pharmaceutical products and studies related to the blood flow model etc.

2. Materials and Methods

2.1 Mathematical formulation

We investigate double-dimensional steady incompressible leaning MHD Casson fluid stream on a two unlike plane face likewise permeable and a liquefying plane with first and second order pace slip, non-linear emission, non-even temperature source and non-linear chemical response. Let surface is extending along the x axis with extending velocity bx. The diagram in Fig. 1a. gives a pictorial view of this problem.

The continuity, velocity, heat, and mass equations are given by

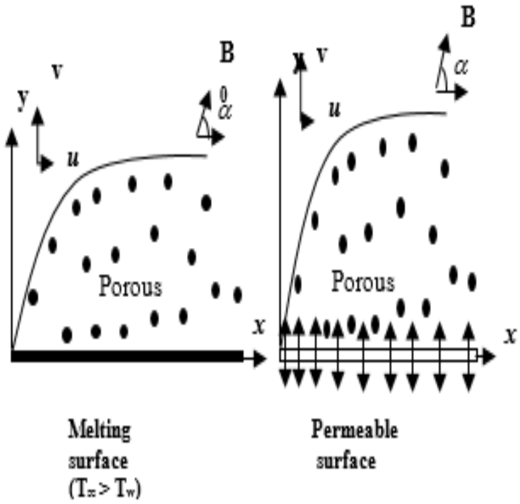

Fig. 1a. Physical diagram of the problem 2.2 Equations.

$$\frac{\partial u}{\partial x}+\frac{\partial v}{\partial y}=0, \tag{2.1}$$

$$U\frac{\partial u}{\partial x}+V\frac{\partial v}{\partial y}=V\left(1+\frac{1}{\beta}\right)\frac{\partial^2 u}{\partial y^2}+g\beta_T\left(T-T_\infty\right)+ g\beta_C\left(C-C_\infty\right)-\frac{\sigma B_0^2\sin^2\alpha u}{\rho}-\left(1+\frac{1}{\beta}\right)\frac{uv}{K_P}, \tag{2.2}$$

$$U\frac{\partial T}{\partial x}+V\frac{\partial T}{\partial y}=\frac{k}{\rho C_P}\frac{\partial^2 T}{\partial y^2}-\frac{1}{\rho C_P}\frac{\partial q_r}{\partial y}+ \frac{q'''}{\rho C_P}+\frac{\mu}{\rho C_P}\left(1+\frac{1}{\beta}\right)\left(\frac{\partial u}{\partial y}\right)^2+ \frac{\sigma\sin^2\alpha u^2 B_0^2}{\rho C_P}+\frac{DmK_T}{C_S C_P}\left(\frac{\partial T}{\partial y}\right)^2, \tag{2.3}$$

$$U\frac{\partial C}{\partial x}+V\frac{\partial C}{\partial y}=D_m\frac{\partial^2 C}{\partial y^2}-K_r\left(C-C_\infty\right)^n+ \frac{DmK_T}{T_m}\frac{\partial^2 T}{\partial y^2}, \tag{2.4}$$

where $u(x,y)$ and $v(x,y)$ are the flat and upstanding velocity components, ρ: liquid concentration, v: kinematic viscosity, ρC_P: particles heat strength. T: fluid temperature, T_∞: ambient liquid temperature.

Corresponding boundary conditions are:

(1) **For porous surface** [20, 37]

At $y=0$

$$\left\{\begin{array}{c} u=u_w+\left(a_1\dfrac{\partial u}{\partial y}+a_2\dfrac{\partial^2 u}{\partial y^2}\right), v=-v_w \\ T=T_w+b_1\dfrac{\partial T}{\partial y} \\ C=C_w+b_2\dfrac{\partial C}{\partial y} \end{array}\right\} \quad (2.5)$$

at $y\to\infty, u\to 0, T\to T_\infty, C\to C_\infty$ (2.6)

(2) **For melting surface** [22, 32]

At $y=0$

$$\left\{\begin{array}{c} u=u_w+\left(a_1\dfrac{\partial u}{\partial y}+a_2\dfrac{\partial^2 u}{\partial y^2}\right), \\ v=k\dfrac{1}{\left(\rho\left[\beta_m+C_s\left(T_w-T_0\right)\right]\right)}\dfrac{\partial T}{\partial y} \\ T=T_w+b_1\dfrac{\partial T}{\partial y} \\ C=C_w+b_2\dfrac{\partial C}{\partial y} \end{array}\right\} \quad (2.7)$$

at $y\to\infty, u\to 0, T\to T_\infty, C\to C_\infty,$ (2.8)

$u_w=bx$: stretching velocity, v_w: suction/injection velocity, q''': non-uniform heat source

$$q'''=\frac{ku_w(x,t)}{xv}\left[A^*\left(T_w-T_0\right)f'+B^*\left(T-T_\infty\right)\right],$$

in which A^* and B^*: Space and temperature dependent heat source coefficients, respectively. For optical broad boundary surface, we use Rosseland's dissemination appro. for the radiative heat current

$$q_r\left\{q_r=\frac{-4\sigma^*}{3k^*}\frac{\partial T^4}{\partial y}\right\},$$

where σ^* is the Stephan-Boltzmann $\left(5.6697\times10^{-8}w_m^{-2}k^{-4}\right)$ constant, k^* is the Rosseland's mean amalgamation coefficient The expression T^4 due to emission represented by a function of temperature. So that T^4 can be estimated by Taylor series along T_∞ after ignoring the higher order terms as $T^4=4T_\infty^3-3T_\infty^4$. Consequently, by putting

$$\frac{\partial q_r}{\partial y}=\frac{-16\sigma^*T_\infty^3}{3k^*}\frac{\partial^2 T}{\partial y^2},$$

in the energy Eq. (2.3) we get the subsequent equation:

$$u\frac{\partial T}{\partial x}+v\frac{\partial T}{\partial y}=\frac{k}{\rho C_P}\frac{\partial^2 T}{\partial y^2}+\frac{1}{\rho C_P}\frac{16\sigma^*T_\infty^3}{3k^*}\frac{\partial^2 T}{\partial y^2}$$
$$+\frac{1}{\rho C_P}\frac{ku_w(x,t)}{xv}\left[A^*\left(T_w-T_0\right)f'+B^*\left(T-T_\infty\right)\right]+$$
$$\frac{\mu}{\rho C_P}\left(1+\frac{1}{\beta}\right)\left(\frac{\partial u}{\partial y}\right)^2+\frac{\sigma\sin^2\alpha u^2B_0^2}{\rho C_P}\frac{DmK_T}{C_SC_P}\frac{\partial^2 C}{\partial y^2}. \quad (2.9)$$

Solution: To solve the equation, we use following similarity transformation:

$$u=bxf'(\eta),\ v=\sqrt{bv}f(\eta),\ \eta=y\sqrt{\frac{b}{v}},$$

$$\Phi(\eta)=\frac{C-C_\infty}{C_w-C_\infty} \text{ and } \theta(\eta)=\frac{T-T_\infty}{T_w-T_\infty},$$

where the stream function ψ is

$$u=\frac{\partial\psi}{\partial y}, v=\frac{\partial\psi}{\partial x}.$$

Then we get the following non-dimensional form of equation

$$\frac{\left(f'^2+\left(M\sin^2\alpha\right)f'+K_p\left(1+\frac{1}{\beta}\right)f'-ff''-G_r\theta-G_c\phi\right)}{\left(1+\frac{1}{\beta}\right)}, \quad (2.10)$$

$$\theta''=\left(1+\frac{4}{3}R\left[1+(\varepsilon-1)\theta\right]^3\right)^{-1},$$

$$\left\{\begin{matrix} -f\theta'P_r-A^*f'-B^*\theta-E_cP_r\left(1+\frac{1}{\beta}\right)f''^2 \\ -ME_cP_r\sin^2\alpha f'^2-D_uP_r\Phi''- \\ -4R(\varepsilon-1)\left[1+(\varepsilon-1)\theta\right]^2 \end{matrix}\right\}, \quad (2.11)$$

$$\Phi''=-S_c\Phi' f+S_c\Phi^n K-S_cS_r\theta''. \quad (2.12)$$

The corresponding transformed boundary conditions are

(1) For porous surface

At $\eta=0$,

$$\left\{\begin{matrix} f(\eta)=S, \\ f'(\eta)=1+\left(1+\frac{1}{\beta}\right)\left(L_1f''(\eta)+L_2f'''(\eta)\right) \\ \theta(\eta)=1+\theta'(\eta)\delta_1,\ \Phi(\eta)=1+\Phi'(\eta)\delta_2 \end{matrix}\right\}, \quad (2.13)$$

at $\eta\to\infty$,

$$\left\{f'(\eta)\to 0,\ \theta(\eta)\to 0,\ \Phi(\eta)\to 0\right\}. \quad (2.14)$$

(2) For melting surface

At $\eta\to 0$,

$$\left\{\begin{matrix} f(\eta)=-\frac{Me}{Pr}\theta'(\eta), \\ f'(\eta)=1+\left(1+\frac{1}{\beta}\right)\left(L_1f''(\eta)+L_2f'''(\eta)\right) \\ \theta(\eta)=1+\theta'(\eta)\delta_1,\ \Phi(\eta)=1+\Phi'(\eta)\delta_2 \end{matrix}\right\}, \quad (2.15)$$

at $\eta\to\infty$,

$$\left\{f'(\eta)\to 0,\ \theta(\eta)\to 0,\ \Phi(\eta)\to 0\right\}. \quad (2.16)$$

where $L_1=a_1\sqrt{b/v}$ first order velocity slip parameter, $L_2=a_2\sqrt{b/v}$ second order velocity slip parameter, $\delta_1=a_1\sqrt{b/v}$ temperature slip parameter, $\delta_2=a_2\sqrt{b/v}$ concentration slip parameter, $Pr=k/\mu C_p$ Prandtl number, $R=\frac{4\sigma T_\infty^3}{kk^*}$ radiation parameter, k^* thermal radiation parameter, $Ec=\frac{U^2}{C_p\left(T_w-T_\infty\right)}$ Eckert number, $M=\frac{\sigma B_0^2}{\sigma b}$ magnetic field parameter, β Casson fluid parameter $Sc=v/D_m$ Schmidt number, C_S the heat capacity of the solid surface, $K_n=\frac{k_n}{b}\left(C_w-C_\infty\right)^{n-1}$ chemical reaction parameter, β_m the latent heat of the fluid, $\varepsilon=\frac{T_w}{T_\infty}$ temperature difference parameter, k thermal conductivity, $K_p=\frac{v}{k_pb}$ porosity parameter, $M_e=\frac{\left(T_w-T_\infty\right)C_p}{\beta_m+C_S\left(T_m-T_0\right)}$ dimensionless melting parameter, temperature of the melting surface where $T_m>T_0$,

$$Re_x^{\frac{1}{2}}C_f=\left(1+\frac{1}{\beta}\right)f''(0),$$

$$Nu_xRe_x^{-\frac{1}{2}}=-\left(1+\frac{4R}{3}\varepsilon^3\right)\theta',$$

$$Sh_xRe_x^{-\frac{1}{2}}=-\Phi'(0).$$

Skin friction coefficient, Nusselt number, Mass transfer coefficients are given as below

$$Re_x^{\frac{1}{2}}C_f=\left(1+\frac{1}{\beta}\right)f''(0),$$

$$Nu_xRe_x^{-\frac{1}{2}}=-\left(1+\frac{4R}{3}\varepsilon^3\right)\theta',$$

$$Sh_xRe_x^{-\frac{1}{2}}=-\Phi'(0).$$

3. Results and Discussion

The system of ode (2.1) to (2.4) with corresponding boundary conditions are solved numerically using bvp4c method in MATLAB. All the results are found accurate as they satisfy the final boundary conditions and are compared with the results of Jain et al. [15].The fixed values of the governing parameters are taken as $\beta = 0.5, M = 1, Sr = 0.1, Pr = 0.2, Du = 0.1,$ $Gr = 0.1, Gc = 0.1, Sc = 2, \eta = 1$ and $Kp = 3.$ Figs. 1, 2, and 3 depict the effect of Casson parameter on velocity, temperature, and concentration profiles. It is found that the velocity and temperature profile reduce but concentration profile increases as the Casson parameter increases. It is observed that as the Casson parameter increases the boundary layer thickness also increases so the resistance in velocity appears for both boundary conditions. Figs. 4-6 indicates that as Dufour parameterincreases all three profiles and shows increment with both boundary conditions. Figs. 7-9 shows that with both the boundary conditions increment in Eckert no. give rise to all three profiles. It is seen that as the Eckert number increases. It is significant the internal friction and this gives rise to the self-heating of the fluid and the temperature profile rises. Figs. 10-15 depict that in presence of both boundary conditions increment in thermal Grashof number give rise to velocity profile but temperature and concentration both profiles decrease. it is due to as the thermal Grashof number is high it gives add in thermal energy which give relation to the inter molecule bound and the velocity profile rises. In Figs. 16-17 and 18 showing the effect of permeability parameter along with melting and porous surface boundary condition on all three-velocity heat and mass profiles but it retarded the concentration profile. Figs. 19-21 signifies the effect of magnetic parameters on all three profiles in presence of both the boundary conditions. It shows that increasing the value of magnetic parameter leads to the decreasing velocity but rise in both temperature and concentration profile. It is due to the rise in magnetic field that gives birth to a resisting force called Lorentz force which restricts the fluid motion. Figs. 25-26 describes the impact of increment of Soret number on velocity and temperature profiles and shows that as we increase the solid number velocity profile also increases but temperature profile is reducing.

Table 1. For Porous surface.

M	Kp	Gr	Gc	Ec	Du	Sr	$\left(1+\frac{1}{\beta}\right)f''(0)$	$-\left(1+\frac{4R}{3}\varepsilon^3\right)\theta'$	Φ'
1	0.5	0.1	0.1	0.2	0.1	0.1	-0.6637	-0.7004	-1.685
2	0.5	0.1	0.1	0.2	0.1	0.1	-0.6821	-0.6734	-1.642
5	0.5	0.1	0.1	0.2	0.1	0.1	-0.7055	-0.6304	-1.547
1	**0**	0.1	0.1	0.2	0.1	0.1	-0.6163	-0.7238	-1.775
1	**0.5**	0.1	0.1	0.2	0.1	0.1	-0.6637	-0.7004	-1.685
1	**1.5**	0.1	0.1	0.2	0.1	0.1	-0.7014	-0.6715	-1.567
1	0.5	**0.1**	0.1	0.2	0.1	0.1	-0.6637	-0.7004	-1.685
1	0.5	**0.5**	0.1	0.2	0.1	0.1	-0.4897	-0.7286	-1.695
1	0.5	**1.5**	0.1	0.2	0.1	0.1	-0.5444	-0.7476	-1.907
1	0.5	0.1	**0.1**	0.2	0.1	0.1	-0.6637	-0.7004	-1.685
1	0.5	0.1	**0.5**	0.2	0.1	0.1	-0.6444	-0.7123	-1.755
1	0.5	0.1	**1.5**	0.2	0.1	0.1	-0.6212	-0.7208	-1.906
1	0.5	0.1	0.1	**0.2**	0.1	0.1	-0.6637	-0.7004	-1.685
1	0.5	0.1	0.1	**1**	0.1	0.1	-0.6611	-0.3076	-1.777
1	0.5	0.1	0.1	**2**	0.1	0.1	-0.6578	-0.1997	-1.896
1	0.5	0.1	0.1	0.2	**0.1**	0.1	-0.6637	-0.7004	-1.685

1	0.5	0.1	0.1	0.2	**0.5**	0.1	-0.6554	-0.3662	-1.934
1	0.5	0.1	0.1	0.2	**1**	0.1	-0.6423	2.636	-2.47
1	0.5	0.1	0.1	0.2	0.1	**0.1**	-0.6637	-0.7004	-1.685
1	0.5	0.1	0.1	0.2	0.1	**0.5**	-0.6595	-0.7785	-1.144
1	0.5	0.1	0.1	0.2	0.1	**1**	-.6545	-0.9095	-0.2152

Table 2. For melting surface.

M	Kp	Gr	Gc	Ec	Du	Sr	$\left(1+\frac{1}{\beta}\right)f''(0)$	$-\left(1+\frac{4R}{3}\varepsilon^3\right)\theta'$	Φ'
1	0.5	0.1	0.1	0.2	0.1	0.1	-0.6291	-0.3829	-1.02
2	0.5	0.1	0.1	0.2	0.1	0.1	-0.6537	-0.3357	-0.9623
5	0.5	0.1	0.1	0.2	0.1	0.1	-0.6912	-0.2554	-0.8491
1	**0**	0.1	0.1	0.2	0.1	0.1	-0.6192	-0.4249	-1.149
1	**0.5**	0.1	0.1	0.2	0.1	0.1	-0.6291	-0.3829	-1.02
1	**1.5**	0.1	0.1	0.2	0.1	0.1	-0.6839	-0.3271	-0.8874
1	0.5	**0.1**	0.1	0.2	0.1	0.1	-0.6291	-0.3829	-1.02
1	0.5	**0.5**	0.1	0.2	0.1	0.1	-0.6832	-0.3798	-1.043
1	0.5	**1.5**	0.1	0.2	0.1	0.1	-0.5265	-0.4739	-1.295
1	0.5	0.1	**0.1**	0.2	0.1	0.1	-0.6291	-0.3829	-1.02
1	0.5	0.1	**0.5**	0.2	0.1	0.1	-0.5902	-0.4136	-1.097
1	0.5	0.1	**1.5**	0.2	0.1	0.1	-0.5284	-0.4485	-1.25
1	0.5	0.1	0.1	**0.2**	0.1	0.1	-0.6291	-0.3829	-1.02
1	0.5	0.1	0.1	**1**	0.1	0.1	-0.6128	-0.1398	-0.9396
1	0.5	0.1	0.1	**2**	0.1	0.1	-0.5909	-0.7899	-0.8592
1	0.5	0.1	0.1	0.2	**0.1**	0.1	-0.6291	-0.3829	-1.02
1	0.5	0.1	0.1	0.2	**0.5**	0.1	-0.6109	0.1395	-0.9361
1	0.5	0.1	0.1	0.2	**1**	0.1	-0.5922	0.6301	0.8653
1	0.5	0.1	0.1	0.2	0.1	**0.1**	-0.6291	-0.3829	-1.02
1	0.5	0.1	0.1	0.2	0.1	**0.5**	-0.6266	-0.4102	-0.902
1	0.5	0.1	0.1	0.2	0.1	**1**	-0.6237	-0.4512	-0.7079

Figure 1: Effect of β on Velocity Profile

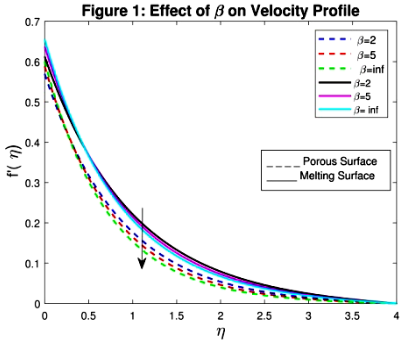

Figure 2: Effect of β on temperature Profile

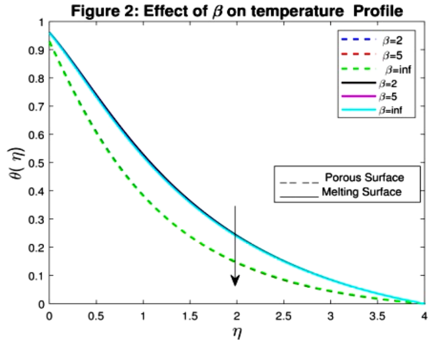

Figure 3: Effect of β on concentration profile

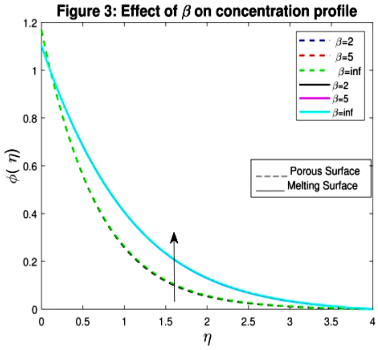

Figure 4: Effect of Du on Velocity Profile

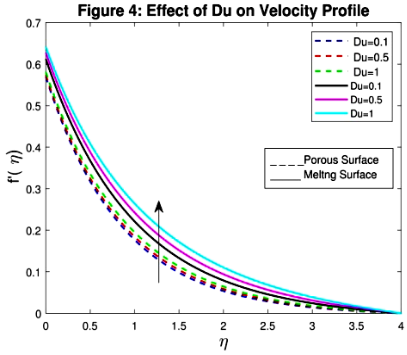

Figure 5: Effect of Du on temperature Profile

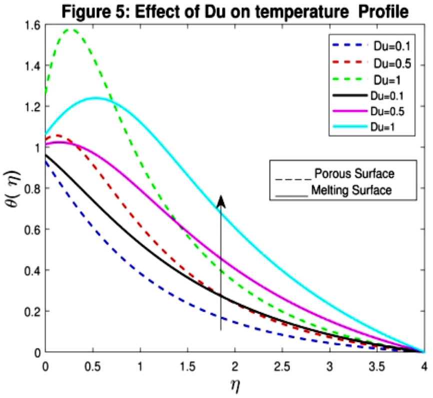

Figure 6: Effect of Du on concentration profile

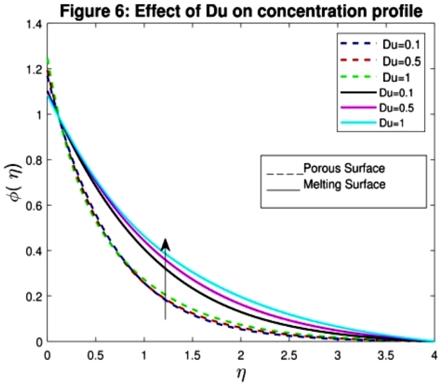

Figure 7: Effect of Ec on Velocity Profile

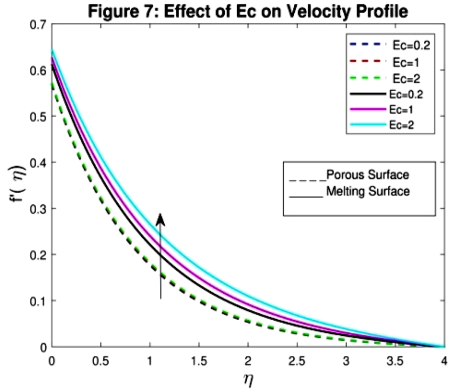

Figure 8: Effect of Ec on temperature Profile

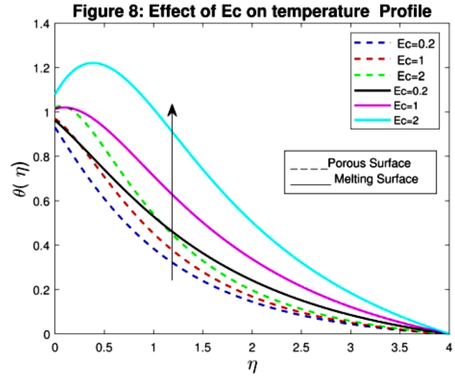

Figure 9: Effect of Ec on concentration profile

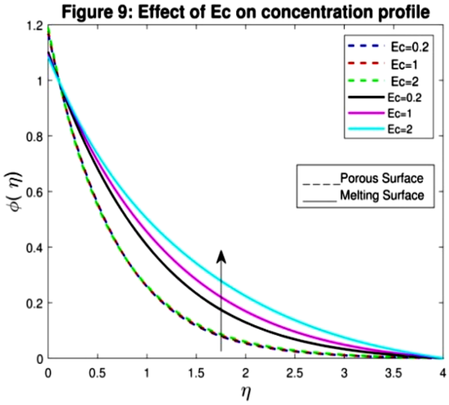

Figure 10: Effect of Gc on Velocity Profile

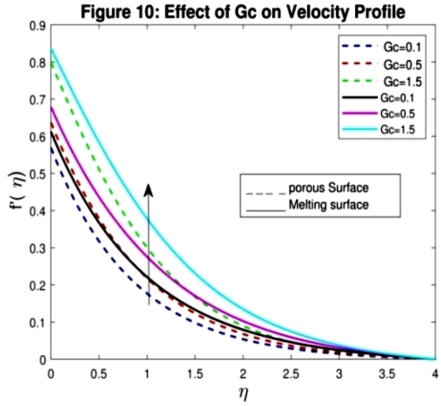

Figure 11: Effect of Gc on temperature Profile

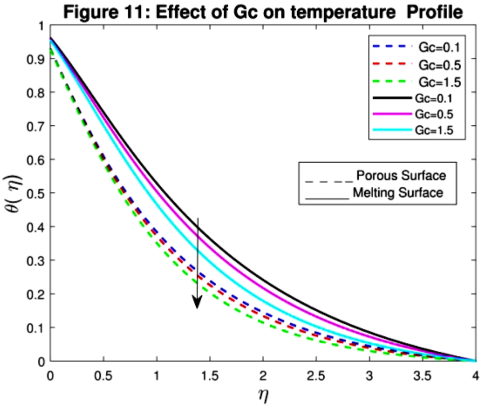

Figure 13: Effect of Gr on Velocity Profile

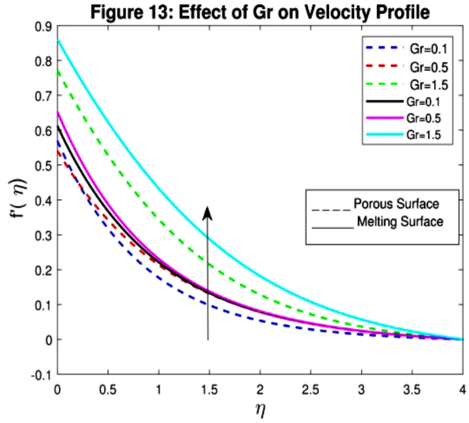

Figure 12: Effect of Gc on concentration profile

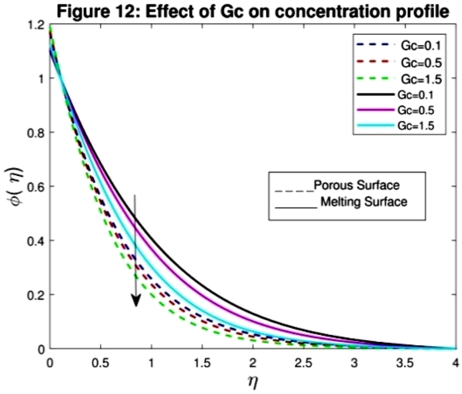

Figure 14: Effect of Gr on temperature Profile

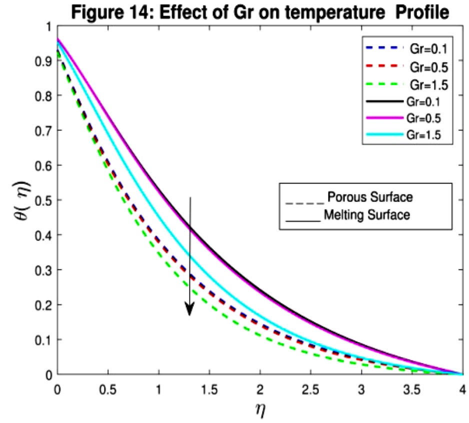

Figure 15: Effect of Gr on concentration profile

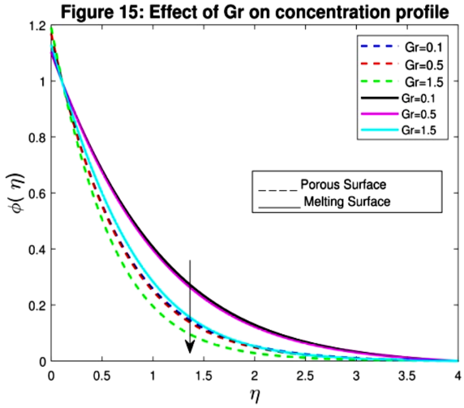

Figure 16: Effect of Kp on Velocity Profile

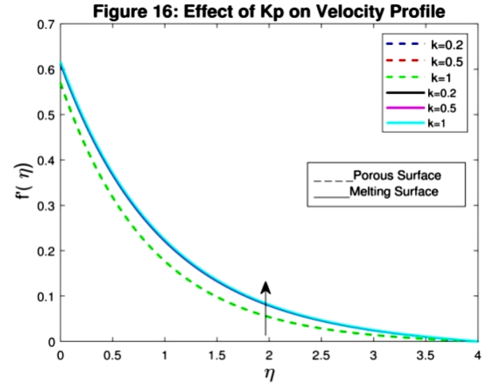

Figure 17: Effect of Kp on temperature Profile

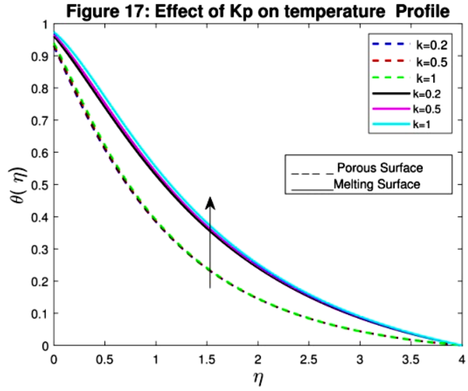

Figure 18: Effect of Kp on concentration profile

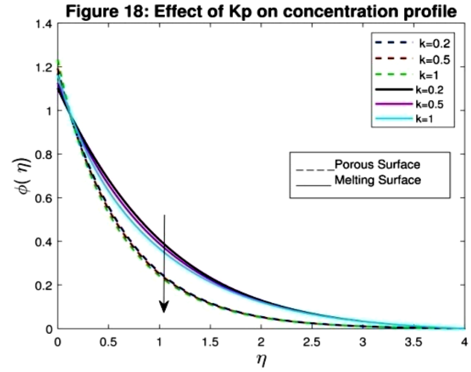

Figure 19: Effect of M on Velocity Profile

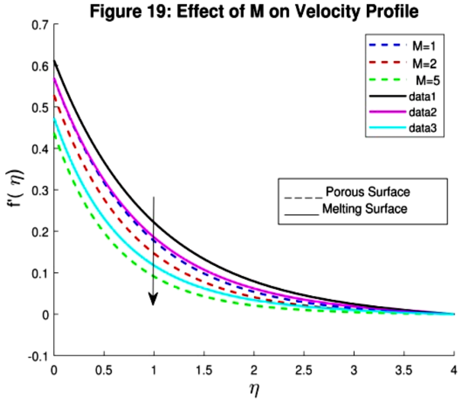

Figure 20: Effect of M on temperature Profile

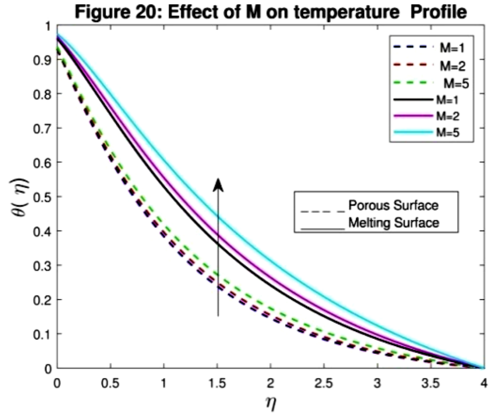

Figure 21: Effect of M on concentration profile

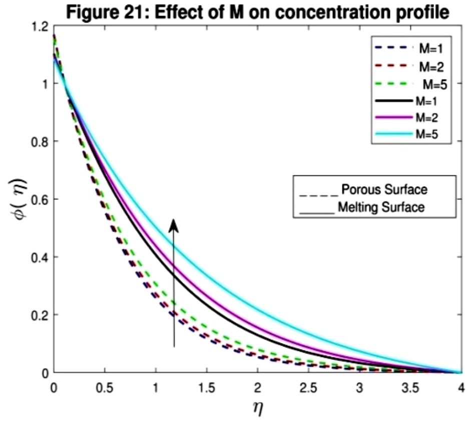

Figure 22: Effect of Me on Velocity Profile

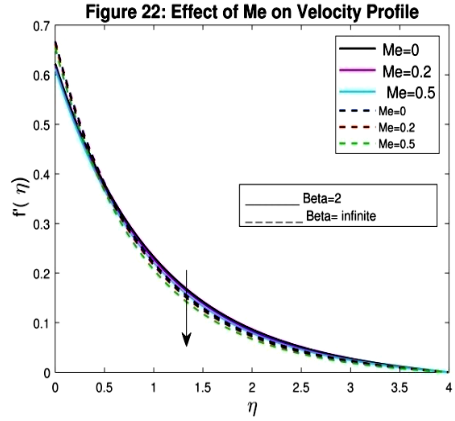

Figure 23: Effect of Me on temperature Profile

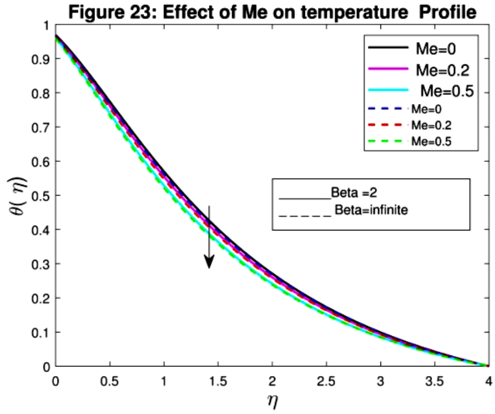

Figure 24: Effect of Me on concentration profile

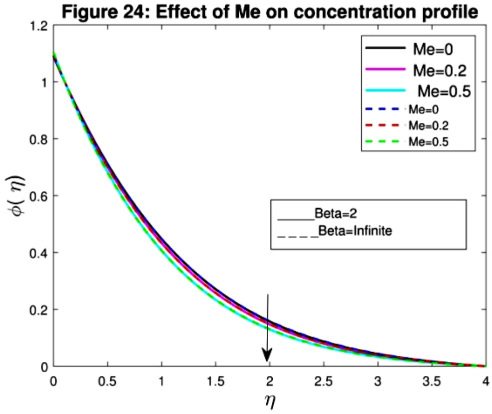

Figure 25: Effect of Sr on Velocity Profile

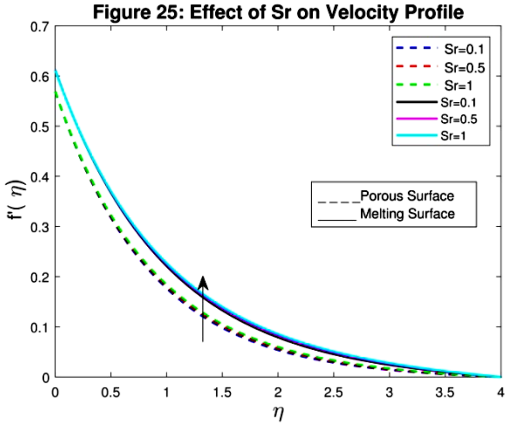

Figure 26: Effect of Sr on temperature Profile

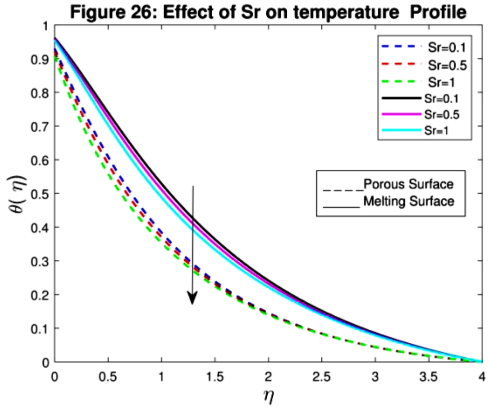

4. Conclusion

The remarkable points of this study are as follows:

1. Velocity profile shows increment when δ_1 temperature slip parameter, δ_2 concentration slip parameter, Du Dufour Number, Ec Eckert number, Gc concentration Grashof Number, Gr velocity Grashof Number, Kp porosity parameter, Sc Schmidt number, Sr sorret number increases and reduces wheh α inclination angle, β Casson fluid parameter, K chemical reaction parameter, L_1 first order velocity slip parameter, M magnetic parameter, Me dimensionless melting parameter, Pr Prandtl number, R radiation parameter, S porous surface parameter for both the boundaries.
2. Energy profile increases with the increment of Du Dufour Number, Ec Eckert number, Kp porosity parameter, M magnetic parameter and shows reduction with increment in β Casson fluid parameter, Gc concentration Grashof Number, Gr velocity GrashofNumber, Me dimensionless melting parameter and Sr sorret number for both the boundaries.

3. Mass profile rises when Du Dufour Number, Ec Eckert number, β Casson fluid parameter and M magnetic parameter rises whereas this profile reduces with increase in Gc concentration Grashof Number, Gr velocity Grashof Number , Me dimensionless melting parameter and Kp porosity parameter for both the boundaries.

References

[1] Andersson H., Hansen O., Holmedalf B., Diffusion of a chemically reactive species from a stretching sheet, ht. J. Hed Mass Transfer.1994; 37:659-64.

[2] Prasad KV., Sujatha A., Vajravelu K. and Pop I.MHD flow and heat transfer of a UCM fluid over a stretching surface with variable thermo

[3] Mukhopadhyay S.,Arif MG. and Ali MWP. Effects of transpiration on unsteady MHD flow of an upper convected Maxwell (UCM) fluid passing through a stretching surface in the presence of a first order chemical reaction. Chinese Physical Society and IOP Publishing Ltd 2013.

[4] Nadeem S., Hussain ST. Flow and heat transfer analysis of Williamson nanofluid, ApplNanosci 2014;4:1005-12.

[5] Krishnamurthy MR., Prasanna kumara BC., Gireesha BJ., Gorla RSR. Effect of chemical reaction on MHD boundary layer flow and melting heat transfer of Williamson nanofluid in porous medium. Engineering Science and Technology, an International Journal 2016;19:53-61.

[6] Kumar PS., Gangadhar K. Effect of chemical reaction on slip flow of MHD Casson fluid over a stretching sheet with heat and mass transfer. Advances in Applied Science Research 2015; 6:205-23.

[7] Megahed AM., MHD viscous Casson fluid flow and heat transfer with second-order slip velocity and thermal slip over a permeable stretching sheet in the presence of internal heat generation/absorption and thermal radiation, Eur. Phys. J. Plus 2015;130:1-17.

[8] Nadeem S. , Mehmood R. and Akbar NA. Partial slip effect on non-aligned stagnation point nanofluid over a stretching convective surface. Chin. Phys. B 2015; 24:1-8.

[9] Ramesh K., Devakar M. Some analytical solutions for flows of Casson fluid with slip boundary conditions. Ain Shams Engineering Journal 2015;6:967-75.

[10] Kataria, Patel HR. Soret and heat generation effects on MHD Casson fluid flow past an oscillating vertical plate embedded through porous medium. Alexandria Engineering Journal 2016;55:2125-37.

[11] Nagendramma V., Kumar RVMSSK., Prasad P. , Leelaratnam A., and Varma SVK. Multiple Slips and Thermophoresis Effects of Maxwell Nanofluid Over a Permeable Stretching Surface in the Presence of Radiation and Dissipation. Journal of Nano fluids 2016; 5:1-9.

[12] Raju C.S.K., Sandeep N., Saleem S. Effects of induced magnetic field and homogeneous–heterogeneous reactions on stagnation flow of a Casson fluid, Engineering Science and Technology, an International Journal 2016;19:875-87.

[13] Sulochana C., kumar AGP., Sandeep N. Similarity solution of 3D Casson nanofluid flow over a stretching sheet

with convective boundary conditions. Journal of the Nigerian Mathematical Society 2016;35:128-41.

[14] Kumar TP. and Gangadhar K. Slip Flow of a Casson Fluid Flow over an Exponentially Stretching Surface and Heat and Mass Transfer. International Research Journal of Engineering and Technology (IRJET) 2015; 02:2040-48.

[15] Jain S., Choudhary R. Combined Effects of Suction/Injection on MHD Boundary Layer Flow of Nano fluid over a Horizontal Permeable Cylinder with Radiation. Jour of Adv Research in Dynamical & Control Systems 2017;11.

[16] Jain, S., Parmar, A. Comparative study of flow and heat transfer behaviour of Newtonian and non-Newtonian fluids over a permeable stretching surface. Glob stochastic Anal. SI 2017; 41-50.

[17] Jain, S., Parmar, A. Multiple slip effects on inclined MHD Casson fluid flow over a permeable stretching surface and a melting surface. International Journal of Heat and Technology 2018; 36:585-94.

[18] Jain S. and Bohra S. Heat and mass transfer over a three-dimensional inclined non-linear stretching sheet with convective boundary conditions. Indian Journal of Pure & Applied Physics 2017; 55:847-56.

[19] Raju CSK., Priyadarshini P.,Ibrahim SM. Multiple Slip and Cross Diffusion on MHD Carreau–Cassonfluid over a Slendering Sheet with Non-uniform Heat Source/Sink, Int. J. Appl. Comput. Math 2017:1-22.

[20] Parmar A., MHD Falkner–Skan Flow of Casson Fluid Flow and Heat Transfer with Variable Property Past a Moving Wedge. Int. J. Appl. Comput. Math 2017:1

[21] Rajani D., Hemalatha K., Madhavi MVDNS. Effects Of Higher Order Chemical Reactions and Slip Boundary Conditions on Nano fluid Flow. Int. Journal of Engineering Research and Application 2017;7:36-45.

[22] Sivakumar N., Prasad PDB , Raju CSK., Varma SVK., Shehzad SA., Partial slip and dissipation on MHD radiative ferro-fluid over a non-linear permeable convectively heated stretching sheet. Results in Physics 2017; 7:1940-9.

[23] Arifuzzaman SM., Khan MS., Mehedi MFU., Rana BMJ., Ahmmed SF. Chemically reactive and naturally convective high speed MHD fluid flow through an oscillatory vertical porous plate with heat and radiation absorption effect. Engineering Science and Technology, an International Journal 2018;21:215-28.

[24] Yahaya RI., Arifin NM., Isa SSPM. Stability Analysis on Magnetohydrodynamic Flow of Casson Fluid over a Shrinking Sheet with Homogeneous-Heterogeneous Reactions. Entropy 2018;20:652.

[25] Ajala OA., Abimbade SF., Gbadeyan OD. Waheed A. A Magnetohydrodynamic Fluid Flow over an Upper Horizontal Surface of a Paraboloid of Revolution. American International Journal of Research in Science, Technology, Engineering & Mathematics 2019; 25: 71-6.

[26] Das M., Mahanta G., Shaw S., Parida S.B. Unsteady MHD chemically reactive double-diffusive Casson fluid past a flat plate in porous medium with heat and mass transfer. Heat Transfer-Asian Res. 2019;48:1761-77.

[27] Waini I. , Ishak A., Pop I. Unsteady flow and heat transfer past a stretching/shrinking sheet in a hybrid nano fluid. International Journal of Heat and Mass Transfer 2019;136: 288-97.

[28] Asogwa KK. and Ibe AA., A Study of MHD Casson Fluid Flow over a Permeable Stretching Sheet with Heat and Mass Transfer. Journal of Engineering Research and Reports 2020; 16:10-25.

[29] Hafidzuddin H.E., Idris M.N. and Arifin N.M. MHD Casson Fluid Flow over a Non-Linear Stretching/Shrinking Sheet with Suction and Slip Boundary Condition. ASM Science Journal 2020;13:1-7.

[30] Khana U., Zaib A., Khan I., Nisar K.S. Activation energy on MHD flow of titanium alloy (Ti6Al4V) nano particle along with a cross flow and stream wise direction with binary chemical reaction and non-linear radiation: Dual Solutions. Journal of Materials Research and Technology2020; 9: 188-99.

[31] Palani S., Kumar BR., Kameswaran PK. Unsteady MHD flow of an UCM fluid over a stretching surface with higher order chemical reaction. Ain Shams Eng J;2016:1

[32] Rasool G., Shafiq A., Khan I. et al. Entropy Generation and Consequences of MHD in Darcy–Forchheimer Nanofluid Flow Bounded by Non-Linearly Stretching Surface. Symmetry 2020; 12:1-23

[33] Bilal S., Shah I.A., Akgu A., Nisar K.S., Khan I., Khashan M.M., Yahia I.S. Finite difference simulations for magnetically effected swirling flow of Newtonian liquid induced by porous disk with inclusion of thermophoretic particles diffusion. Alexandria Eng. J.2021; 25:32-45.

[34] Hussain S.M., Jamshed W., Kumar V. et al. Computational analysis of thermal energy distribution of electromagnetic Casson nanofluid across stretched sheet: Shape factor effectiveness of solid particles. Energy Reports 2021; 7 :7460-77.

[35] JamshedW., AkgülE.K. and Nisar K.S. Keller box study for inclined magnetically driven Casson nanofluid over a stretching sheet: single phase model.Physica Scripta 2021; 96.

[36] Saleem M., Tufail MN. and Chaudhary QA. Unsteady MHD Casson fluid flow with heat transfer passed over a porous rigid plate with stagnation point flow: Two-parameter Lie scaling approach. Pramana – J. Phys. 2021;28:1-9.

[37] Shoaib M., Zubair G., Nisar K.S. et al. Ohmic heating effects and entropy generation for nanofluidic system of Ree-Eyring fluid: Intelligent computing paradigm. International Communications In Heat And Mass Transfer 2021; 129.

[38] Parvin S., Isa SSPM., Arifin NM., Ali FM., The Magnetohydrodynamics Casson Fluid Flow, Heat and Mass Transfer Due to the Presence of Assisting Flow and Buoyancy Ratio Parameters. CFD Letters 2020;12: 64

[39] Bhattacharya K. Boundary layer stagnation point flow of Casson fluid and heat transfer towards a shrinking/stretching sheet. Front Heat Mass Transf 2013; 4: 1-9.